AFRL-RZ-WP-TP-2010-2190

EFFECT OF COPPER ADDITION ON CRYSTALLIZATION AND PROPERTIES OF HAFNIUM CONTAINING HITPERM ALLOYS (POSTPRINT)

L. Christy and J.C. Horwath

Mechanical Energy Conversion Branch
Energy/Power/Thermal Division

Z. Turgut and M. Huang

UES Inc.

OCTOBER 2009

AIR FORCE RESEARCH LABORATORY
PROPULSION DIRECTORATE
WRIGHT-PATTERSON AIR FORCE BASE, OH 45433-7251
AIR FORCE MATERIEL COMMAND
UNITED STATES AIR FORCE

REPORT DOCUMENTATION PAGE

Form Approved
OMB No. 0704-0188

1. REPORT DATE *(DD-MM-YY)*	2. REPORT TYPE	3. DATES COVERED *(From - To)*
October 2009	Journal Article Postprint	31 October 2008 – 31 October 2009

4. TITLE AND SUBTITLE
EFFECT OF COPPER ADDITION ON CRYSTALLIZATION AND PROPERTIES OF HAFNIUM CONTAINING HITPERM ALLOYS (POSTPRINT)

5a. CONTRACT NUMBER
In-house

5b. GRANT NUMBER

5c. PROGRAM ELEMENT NUMBER
62203F

6. AUTHOR(S)
L. Christy and J.C. Horwath (AFRL/RZPG)
Z. Turgut and M. Huang (UES Inc.)

5d. PROJECT NUMBER
3145

5e. TASK NUMBER
01

5f. WORK UNIT NUMBER
314501CG

7. PERFORMING ORGANIZATION NAME(S) AND ADDRESS(ES)
Mechanical Energy Conversion Branch (AFRL/RZPG)
Energy/Power/Thermal Division
Air Force Research Laboratory, Propulsion Directorate
Wright-Patterson Air Force Base, OH 45433-7251
Air Force Materiel Command, United States Air Force

UES Inc.
4401 Dayton-Xenia Road
Dayton, OH 45432

8. PERFORMING ORGANIZATION REPORT NUMBER
AFRL-RZ-WP-TP-2010-2190

9. SPONSORING/MONITORING AGENCY NAME(S) AND ADDRESS(ES)
Air Force Research Laboratory
Propulsion Directorate
Wright-Patterson Air Force Base, OH 45433-7251
Air Force Materiel Command
United States Air Force

10. SPONSORING/MONITORING AGENCY ACRONYM(S)
AFRL/RZPG

11. SPONSORING/MONITORING AGENCY REPORT NUMBER(S)
AFRL-RZ-WP-TP-2010-2190

12. DISTRIBUTION/AVAILABILITY STATEMENT
Approved for public release; distribution unlimited.

13. SUPPLEMENTARY NOTES
Journal article published in the *Applied Physics Letters*, Vol. 107 (2010). The journal article contains color.
PA Case Number: 88ABW-2009-4770; Clearance Date: 18 Nov 2009.

14. ABSTRACT
This paper presents properties and nanocrystallization characteristics of HITPERM based $Fe_{68.8}Co_{17.2}Hf_7Cu_1B_6$ and $Fe_{69.6}Co_{17.4}Hf_7B_6$ alloys. Both alloys differing only in copper content were subjected to series of characterizations in order to study the effect of copper. Evolution of magnetic properties as a function time has been investigated by isothermal annealing experiments and optimum annealing conditions of amorphous precursors have been reported. Resulting magnetic properties (AC and DC) measured at room temperature are presented. Nanocrystallization kinetics studied by using time dependant magnetization measurements was discussed in the framework of Johnson-Mehl-Avrami model. Results of thermal stability measurements conducted in air at 500 K for up to 1000 hours are reported.

15. SUBJECT TERMS
iron cobalt, FeCo, soft magnetic materials

16. SECURITY CLASSIFICATION OF:			17. LIMITATION OF ABSTRACT:	18. NUMBER OF PAGES	19a. NAME OF RESPONSIBLE PERSON (Monitor)
a. REPORT	b. ABSTRACT	c. THIS PAGE			John C. Horwath
Unclassified	Unclassified	Unclassified	SAR	12	19b. TELEPHONE NUMBER *(Include Area Code)* N/A

Standard Form 298 (Rev. 8-98)
Prescribed by ANSI Std. Z39-18

Effect of copper addition on crystallization and properties of hafnium containing HITPERM alloys (invited)

Z. Turgut,[1,2,a] L. Christy,[2] M. Huang,[1,2] and J. C. Horwath[2]
[1]*AFRL, Wright-Patterson AFB, Ohio 45433, USA*
[2]*UES Inc., Wright-Patterson AFB, Ohio 45433, USA*

(Presented 19 January 2010; received 30 October 2009; accepted 17 February 2010; published online 4 May 2010)

This paper presents properties and nanocrystallization characteristics of HITPERM based $Fe_{68.8}Co_{17.2}Hf_7Cu_1B_6$ and $Fe_{69.6}Co_{17.4}Hf_7B_6$ alloys. Both alloys differing only in copper content were subjected to series of characterizations in order to study the effect of copper. Evolution of magnetic properties as a function time has been investigated by isothermal annealing experiments and optimum annealing conditions of amorphous precursors have been reported. Resulting magnetic properties (ac and dc) measured at room temperature are presented. Nanocrystallization kinetics studied by using time dependant magnetization measurements was discussed in the framework of Johnson–Mehl–Avrami model. Results of thermal stability measurements conducted in air at 500 K for up to 1000 h are reported. © *2010 American Institute of Physics*. [doi:10.1063/1.3368723]

I. INTRODUCTION

HITPERM alloys, $(Fe_xCo_{1-x})_{88}Zr_7B_4Cu_1$, developed a decade ago by Willard *et al.*[1] for high temperatures, continue to be an active research area. Developed as a derivative to the Fe–Zr–B based nanocrystalline NANOPERM alloys, earlier compositions of the HITPERM alloys were magnetically harder than their NANOPERM or FINEMET (FeSiBNbCu) counterparts. Hafnium containing HITPERM alloy was first studied by Iwanabe *et al.*,[2] who reported coercivity values around 300 A/m. Over the years, compositional refinements brought this class of alloys on par with NANOPERM and FINEMET with the capability of operating at higher temperatures. A detailed literature search on alloy chemistries reveal the following effects of alloying elements.[3–9]

(1) Increased cobalt content increases coercivity; from 0% to 30% Co, coercivity values are low and beyond 30% Co, coercivity increases monotonically.
(2) Among Zr, Hf, and Nb, hafnium is the most effective element suppressing grain growth, thus increasing thermal stability.
(3) Chromium and vanadium additions have detrimental effect on magnetic properties.
(4) Combined Nb–Zr additions are most effective in increasing electrical resistivity.
(5) Copper additions (1 at. %) do not effect final grain size but lower primary and secondary crystallization temperatures along with the Curie temperature of the amorphous phase. Cu free compositions are also magnetically softer.
(6) Silicon additions increase oxidation resistance.

We are studying this alloy system as an inductive component for a high power high performance interleaved power converter that is designed for a continuous operation at 473 K. Although the operating frequencies of metallic nanocrystalline cores are lower than that of ferrites, the higher saturation magnetization and wider operating temperature ranges can easily compensate the limitation of operating frequencies and bring out greater benefits.

II. EXPERIMENTAL PROCEDURES

Two alloy ingots with nominal compositions of $Fe_{68.8}Co_{17.2}Hf_7Cu_1B_6$ and $Fe_{69.6}Co_{17.4}Hf_7B_6$ were prepared by arc melting and melt spun using a single roller melt spinner at a wheel speed of 35 m/s. Crystallization behavior of the samples was studied by differential scanning calorimetry (DSC) and a vibrating sample magnetometer (VSM) equipped with a 1275 K high temperature furnace. Magnetic measurements were carried out using the VSM, and an ac hysteresisgraph. Structural characterizations were studied using x-ray diffraction (XRD) with Cu $K\alpha$ radiation. A scanning electron microscope (SEM) was used for imaging.

III. AS-CAST RIBBONS

Melt spinning in argon atmosphere yielded ~3 mm wide continuous ribbons with average thicknesses of ~20 μm. XRD patterns taken on the free surface of the ribbons indicated a weak crystalline peak corresponding to the diffractions from (200) planes of the bcc FeCo phase (Fig. 1). A missing (110) reflection that is proportional to the intensity of the (200) peaks ($I_{(110)}/I_{(200)} \sim 7$ in a randomly oriented fully crystalline FeCo system) clearly indicates presence of a texture.

Thermomagnetic $M(T)$ measurements revealed that both alloys were ferromagnetic in as-cast state with different Curie (T_c) and crystallization (T_{x1}) temperatures. Figure 2 shows that the magnetization decreases monotonically as the amorphous phases approach their respective Curie temperatures. The copper free alloy exhibited a curie temperature of 683 K while the T_c of the copper containing alloy was 671 K.

[a]Electronic mail: zafer.turgut@wpafb.af.mil.

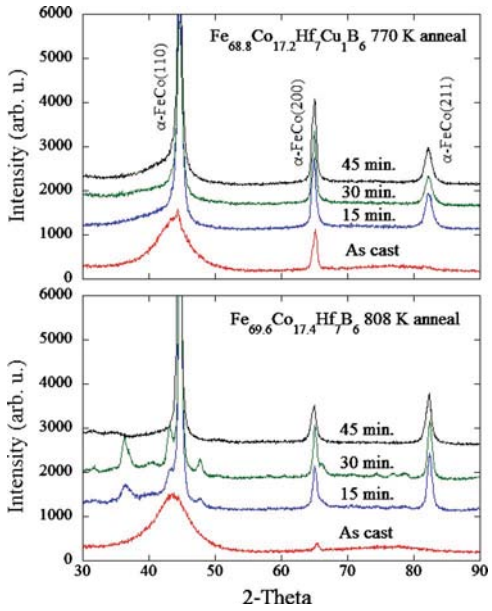

FIG. 1. (Color online) XRD patterns of as-cast and isothermally annealed $Fe_{68.8}Co_{17.2}Hf_7Cu_1B_6$ (top) and $Fe_{69.6}Co_{17.4}Hf_7B_6$ (bottom) alloys for specified annealing times.

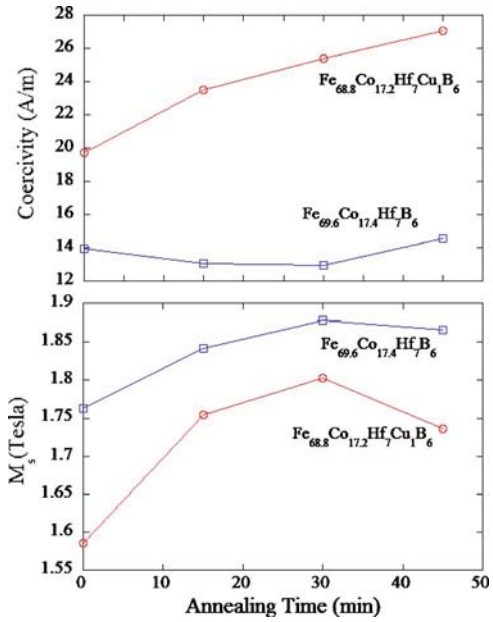

FIG. 3. (Color online) Effect of annealing time on the coercivity and saturation magnetization of Cu-free and Cu-containing alloys annealed at 808 and 770 K, respectively.

Despite the presence of some crystalline FeCo phase in the as-cast state, both samples lost almost all of their magnetization once the temperature increased beyond the T_c of the amorphous phase and before any crystallization took place. This may be a result of two things: the volume fraction of the crystalline phase on the free surface is very low or this response may be attributed to the superparamagnetism of the small particles. If the crystalline phase on the surface is in the form of small isolated crystallites embedded in an amorphous matrix, they magnetically decouple and exhibit superparamagnetism once the Curie temperature of the amorphous phase is exceeded. With increasing temperature, the amorphous phase starts to crystallize into a higher Curie temperature FeCo phase. The crystallization temperature of copper free alloy ($T_{x1} \sim 808$ K) was higher than that of copper containing alloy ($T_{x1} \sim 770$ K). Both alloys stayed ferromagnetic up to the bcc to fcc phase transformation temperature ($T_{\alpha \rightarrow \gamma} \sim 1253$ K) of the crystallized FeCo phase. DSC measurements agree well with the above results. DSC measurements also showed different secondary crystallization temperatures (T_{x2}) in which the remaining amorphous phase starts to crystallize into refractory phases. T_{x2} of Cu-containing alloy was 972 K while T_{x2} of Cu-free alloy was significantly higher at 1125 K. This is a clear indication of the fact that presence of Cu promotes the formation of a Hf–B containing refractory phases at lower temperatures. The secondary crystallization temperature is often regarded as the upper limit of use for nanocrystalline materials but long term exposure to lower temperatures may allow for structural changes and precipitate formations limiting the use of these materials to lower temperatures. Copper additions apparently decrease Curie temperature of the amorphous phase and lowers primary and secondary crystallization temperatures.

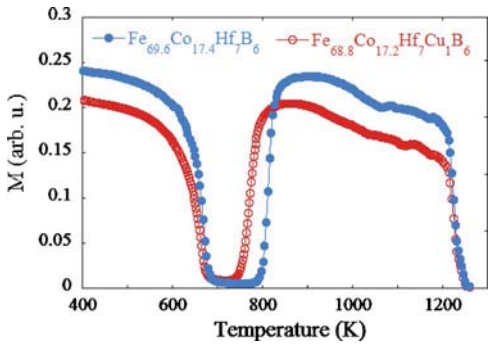

FIG. 2. (Color online) Thermomagnetic $M(T)$ plots of $Fe_{68.8}Co_{17.2}Hf_7Cu_1B_6$ and $Fe_{69.6}Co_{17.4}Hf_7B_6$ alloys measured under an applied field of 1 kOe.

IV. ISOTHERMAL ANNEALING

The two alloys were subjected to an isothermal annealing at their respective crystallization temperatures up to 45 min. Series of samples were annealed in argon atmosphere and the process was interrupted by quenching the samples in ice water. In as-cast state, both alloys were magnetically soft with coercivity (H_c) and saturation magnetization (M_s) values of $H_c = 19.7$ A/m, $M_s = 1.58$ T (copper containing alloy) and $H_c = 13.9$ A/m, $M_s = 1.76$ T (copper free alloy). The M_s values of both alloys first increased upon crystallization and then peaked at 30 min annealing time. Longer holding times for both alloys caused the M_s values to decrease. The coercivity of the copper containing alloy increased upon crystallization and continued to increase as the transformed crystalline volume increased. After 15 min annealing, H_c of the copper free alloy decreased slightly, probably due to elimination of residual stresses that may originate from winding these ribbons into a tape form. After 30 min annealing, coercivity of this alloy started to increase (Fig. 3).

XRD measurements (Fig. 2) taken on wheel surface of the isothermally annealed samples revealed that even after 45

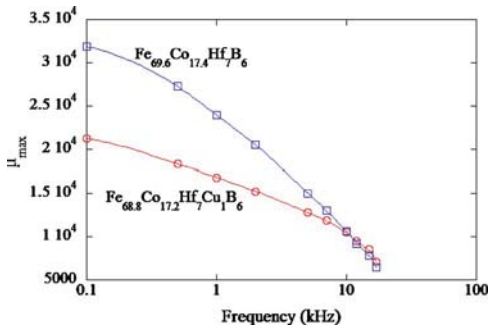

FIG. 4. (Color online) Frequency dependence of maximum permeability for optimally annealed samples.

min annealing, the copper containing alloy exhibited only reflections from the α-FeCo phase. Copper free alloy on the other hand showed an intermediate metastable phase with an undetermined crystal structure along with the α-FeCo phase. This metastable phase that was clearly visible in XRD patterns of 15 min annealed samples grew gradually in volume during 30 min annealing and disappeared in 45 min annealed samples. Repeated experiments confirmed the same results. It is not clear if the formation of the metastable phase is a result of the annealing temperature employed or lack of Cu in this composition, it did not have any deteriorating effect on magnetic properties. One can presume that this phase is ferromagnetic in nature and has comparable magnetic anisotropy to the host α-FeCo phase.

Additionally, the presence of Cu had no effect on the grain size of the two alloys. Using the Scherrer analysis, we estimated an average grain size of 11 nm for both alloys. At all specified annealing times, the grain size was very similar indicating that hafnium is an effective refractory metal in suppressing grain growth. This last observation agrees well with the results of Ping *et al.*,[10] who concluded that Cu additions do not influence the grain size in $Fe_{44}Co_{44}Zr_7Cu_1B_4$ alloys.

Ac measurements taken on 30 min annealed samples showed higher permeability values for copper free alloy than that of copper containing alloy (Fig. 4). At 100 Hz, μ_{max} values for copper free and copper containing alloys were 31900 and 21270, respectively. At 10 kHz, these values reduced to 10682 for the copper free and 10480 for the copper containing alloys. As expected, the copper free alloy showed lower core loss values than the copper containing alloy.

It appears that although the presence of copper has no effect on final grain size, it has a significant effect on magnetic properties. Copper additions increase coercivity and lower saturation magnetization and permeability resulting in higher core loss values.

V. CRYSTALLIZATION KINETICS

As a number of studies indicate, partitioning of alloying elements accompanies the nanocrystallization process in base HITPERM alloys. A primary crystallization phase is identified as α'-(FeCo) phase with an ordered B2 structure while glass forming elements (Zr, Hf, B) are ejected from the primary nanocrystals and enriched in the residual amorphous matrix.

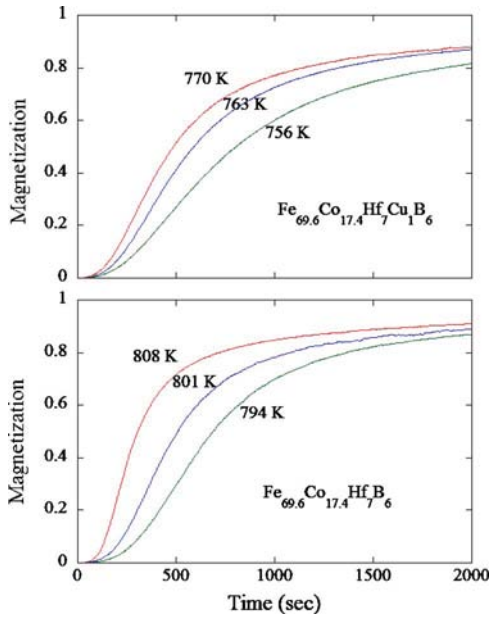

FIG. 5. (Color online) Time dependant normalized magnetization responses of $Fe_{68.8}Co_{17.2}Hf_7Cu_1B_6$ and $Fe_{69.6}Co_{17.4}Hf_7B_6$ alloys taken under 3 kOe applied field.

During isothermal annealing, magnetization (M) increases with time due to crystallization and growth of the nanocrystalline phase. If we assume that the change in magnetization is directly proportional to the volume crystallized, we can define the crystallized volume fraction, $X(t) = M(t)/M(\infty)$ as a function of time dependant magnetization. Time dependant magnetization response of the samples was measured under isothermal conditions at 808, 801, and 794 K for copper free alloy and 770, 763, and 756 K for the copper containing alloy. The highest crystallization temperatures employed for both alloys correspond to the inflection points obtained from the $M(T)$ measurements. Magnetic isotherms that were taken under a 3 KOe applied field and normalized to their saturation value are given in Fig. 5.

The kinetics of the primary crystallization was studied in the framework of the Johnson–Mehl–Avrami (JMA) model. The crystallized volume fraction, $X(t)$ as a function of time, t, is written as

$$X(t) = 1 - \exp(kt^n), \tag{1}$$

where k is a kinetic rate constant and n is the morphology index.

The JMA plots (Fig. 6) obtained for the two compositions at different temperatures are nonlinear but have two linear regions with different slopes. For both alloys, the change in slope from one linear region to another corresponds to a crystallized volume fraction of around $X=0.45$ to 0.55. Morphology indices, n, obtained from the first linear parts of the JMA plots ranged from 2.4 to 2.5 for copper containing alloy and 2.5 to 3.2 for copper free alloy (Table I). These values are consistent with a three-dimensional (3D) nucleation and growth mechanism. The second linear regions, however, exhibited slope values lower than unity indicating a significant slowdown in crystallization rate. These abnormally low values in the later part of the crystallization

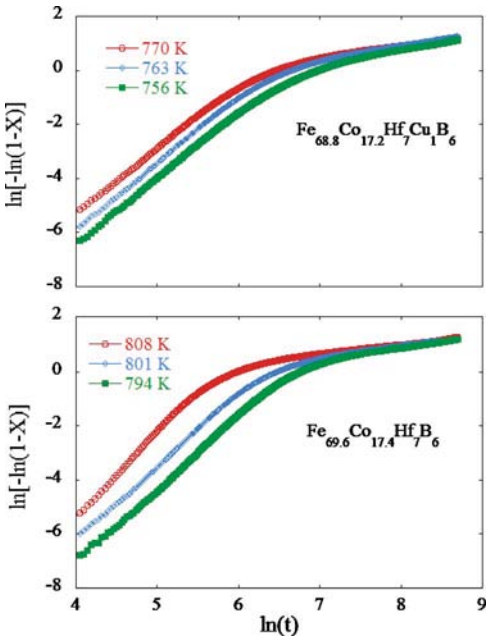

FIG. 6. (Color online) The JMA plots of $\ln[-\ln(1-x)]$ vs $\ln(t)$ for copper containing (top) and copper free (bottom) alloys at given annealing temperatures.

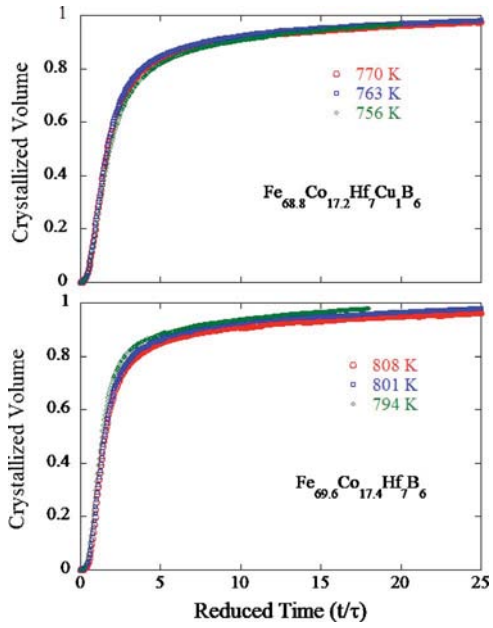

FIG. 7. (Color online) The isothermal magnetization curves plotted in terms of the scaled time t/τ.

process is explained by redistribution of glass forming constituents to the intergranular amorphous phase causing concentration gradients at the age of growing grains and acting as a diffusion barrier to further growth, slowing down the crystallization rate (see e.g., Pradell *et al.*[11] and Hermann *et al.*[12]). At this stage, growth rate is limited by the slowest diffusing constituent. As crystallization proceeds, the growth rate is further reduced by overlapping of diffusion profiles of neighboring grains (soft impingement).

The activation energy (E_a) is calculated using the following Arrhenius type relationship in which the activation energy is expressed in terms of an inflection time, $\tau(T)$, for which dM/dt is maximum and

$$\tau^{-1} = \tau_o^{-1} \exp\left(-\frac{E_a}{k_B T}\right), \tag{2}$$

where k_B is the Boltzman constant and T is the absolute temperature. For each magnetic isotherm, we can experimentally find the time $\tau(T)$ (see Table I) and estimate the E_a from the slope of $\ln(\tau)$ versus $1/(k_B T)$ plots. The activation energies derived from the above linear curve fits were 1.49 eV/atom for the copper containing alloy and 3.9 eV/atom for the copper free alloy. The base HITPERM composition is reported to have an activation energy of 3.8 eV/atom.[13] The lower activation energy obtained for the copper containing alloy correlates well with the lower primary crystallization temperature found for this composition. Although copper is ineffective on determining the final grain size, it is highly effective in reducing the energy barrier to crystallization.

Time evolution of any quantity should be universal when expressed in terms of a scaled time. For each isotherm, if we use the experimentally determined inflection time $\tau(T)$ to define a reduced time axis (t/τ), all the isotherms taken at different temperatures should merge onto a single curve, as illustrated in Fig. 7. The significance of this scaling behavior will not be discussed here in detail (see Ref. 14 and references thereof for a detailed explanation). It basically implies a diminishing nucleation rate over time and a constant velocity isotropic growth until the eventual impingement of the growing nanocrystals. Again, this is consistent with the morphology indices that indicated a 3D nucleation and diffusional growth mechanism.

VI. FRACTURE BEHAVIOR AFTER CRYSTALLIZATION AND SURFACE OXIDATION

Thermal stability studies conducted in air at 500 K for up to 1000 h did not indicate any magnetic property changes. While the two alloys studied were mechanically sound in their as-cast state, they become relatively brittle once they

TABLE I. Morphology index (n) and inflection times (τ) of the two alloy at given temperatures.

$Fe_{68.8}Co_{17.2}Hf_7Cu_1B_6$			$Fe_{69.6}Co_{17.4}Hf_7B_6$		
Temp. (K)	n	τ (s)	Temp. (K)	n	τ (s)
770	2.4	290	808	3.2	199
763	2.5	360	801	2.5	336
756	2.4	444	794	2.7	541

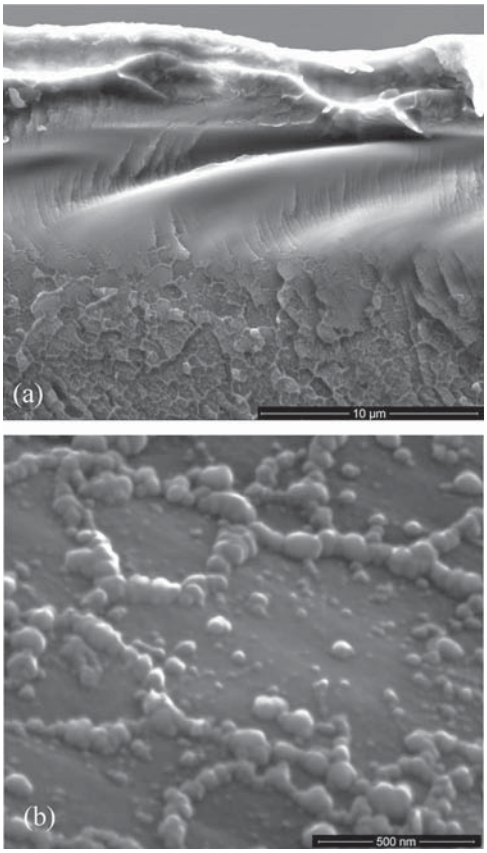

FIG. 8. Fracture surface (a) and surface oxide formation (b) of crystalline $Fe_{68.8}Co_{17.2}Hf_7Cu_1B_6$ alloy aged at 500 K for 1000 h.

are crystallized. The brittle nature after crystallization can be explained by emergence of the intergranular phase that is enriched in glass forming elements during crystallization and growth. Cross sectional fracture surface images of both alloys exhibit two distinct regions with two different fracture modes. An example is given in Fig. 8(a). One half of the ribbon that corresponds to the wheel surface failed by brittle cleavage fracture and the fracture mode changed to a brittle intergranular fracturing for the free surface. The transition from cleavage to intergranular fracture clearly indicates that the wheel surface and the free surface of the ribbons differ in grain sizes.

Isothermal oxidation behavior of FeCo based bulk alloys have been studied by Turgut *et al.*[15] Exposure to air at elevated temperatures leads to selective oxidation of iron and formation of $MO-Fe_2O_3$ type (where M=Co and/or other alloying elements) spinel structures. These surface oxides do not block the inward diffusion of oxygen making the oxidation a continuous process. Also, elements that have lower oxygen affinity than iron or those that are not soluble in the oxide scale tend to increase the oxidation rate. Being heavily alloyed compared to the bulk FeCo alloys, one can expect higher oxidation rates in nanocrystalline alloys. Since no evidence has been found in bulk alloys for grain boundary diffusion of oxygen, finer grain size of nanocrystals should not play a significant role in oxidation of HITPERM alloys. Figure 8(b) shows a SEM surface image of $Fe_{69.6}Co_{17.4}Hf_7B_6$ alloy isothermally annealed at 500 K for 1000 h in air. A network of oxide particles is visible on the surface. The observed relatively low oxidation rate makes these alloys suitable for continuous use at the 473 K.

VII. CONCLUSIONS

Nanocrystallization of two Hf containing Hitperm alloys has been studied. Magnetic properties are found to be optimum after 30 min of crystallization time. Introduction of 1 at. % copper decreases the Curie temperature of the amorphous phase and lowers primary and secondary crystallization temperatures. Although presence of copper has no effect on final grain size, it increases coercivity and lowers saturation magnetization and permeability. Copper is also found to lower the activation energy for nanocrystallization.

[1]M. A. Willard, D. E. Laughlin, M. E. McHenry, D. Thoma, K. Sickafus, J. O. Cross, and V. G. Harris, J. Appl. Phys. **84**, 6773 (1998).
[2]H. Iwanabe, B. Lu, M. E. McHenry, and D. E. Laughlin, J. Appl. Phys. **85**, 4424 (1999).
[3]M. Kowalczyk, J. Ferenc, X. B. Liang, and T. Kulik, J. Magn. Magn. Mater. **304**, e651 (2006).
[4]M. Pekala, M. Kowalczyk, and T. Kulik, Phys. Status Solidi A **203**, 1561 (2006).
[5]Y. Yoshizawa, S. Fujii, D. H. Ping, M. Ohnuma, and K. Hono, Mater. Sci. Eng., A **375-377**, 207 (2004).
[6]J. E. May, M. F. deOliveira, and S. E. Kuri, Mater. Sci. Eng., A **361**, 179 (2003).
[7]T. Kulik, J. Ferenc, A. K. Burian, X. B. Liang, and M. Kowalczyk, J. Alloys Compd. **434-435**, 623 (2007).
[8]X. Liang, T. Kulik, J. Ferenc, and B. Xu, J. Magn. Magn. Mater. **308**, 227 (2007).
[9]K. Pekala, J. Non-Cryst. Solids **354**, 5304 (2008).
[10]D. H. Ping, Y. Q. Wu, K. Hono, M. A. Willard, M. E. McHenry, and D. E. Laughlin, Scr. Mater. **45**, 781 (2001).
[11]T. Pradell, D. Crespo, N. Clavaguera, and M. T. Clavaguera-Mora, J. Phys.: Condens. Matter **10**, 3833 (1998).
[12]H. Hermann, N. Mattern, S. Roth, and P. Uebele, Phys. Rev. B **56**, 13888 (1997).
[13]M. E. McHenry, F. Johnson, H. Okumura, T. Ohkubo, V. R. V. Ramanan, and D. E. Laughlin, Scr. Mater. **48**, 881 (2003).
[14]Y. Yamada, N. Hamaya, J. D. Axe, and S. M. Shapiro, Phys. Rev. Lett. **53**, 1665 (1984).
[15]Z. Turgut, J. C. Horwath, M. Huang and J. E. Coate, J. Appl. Phys. **105**, 07A330 (2009).